Submitted to: Journal of Materials Science: Materials in Medicine

Poly($_L$-lactic acid)/Vaterite Composite Coatings on Metallic Magnesium

Shinya Yamada[1], Akiko Yamamoto[2], Toshihiro Kasuga[1]

[1]*Department of Frontier Materials, Nagoya Institute of Technology, Gokiso-cho, Showa-ku, Nagoya, Aichi, 466-8555, Japan*

[2]*Biometals Group, Biomaterials Unit, Nano-Life Field, International Center for Materials Nanoarchitechtonics (MANA), National Institute for Materials Science (NIMS), 1-1 Namiki, Tsukuba, Ibaraki, 305-0044, Japan*

*Corresponding author

Toshihiro Kasuga

TEL & FAX: +81-52-735-5288

E-mail: kasuga.toshihiro@nitech.ac.jp

Abstract

Poly(L-lactic acid)/vaterite composite materials were coated onto metallic magnesium substrates to control rapid degradation and to improve biocompatibility. Two types of composites were prepared by adding 30 and 60 wt % of vaterite to poly(L-lactic acid) (PLLA). The composite coating layer that contained 30 wt % vaterite in the PLLA matrix had almost no pores on the surface and suppressed the initial rapid degradation of the Mg substrate. After immersion in a culture medium for 7 days, pores of 0.5–1.0 μm in diameter formed on the surface. The composite coating layer that contained 60 wt % vaterite with pores of 1.0–2.0 μm in diameter on the surface did not suppress the degradation of the Mg substrate. During immersion, the pH of the media near the composite coating surfaces was maintained at 7.4–7.5 because of the degradation of PLLA and because the vaterite particles dissolved in the solution. Proliferation of murine osteoblast-like cells (MC3T3-E1) on the substrates was improved using composite coatings. Cells on the coating that contained 60 wt % vaterite had significantly higher proliferation than those on a bare Mg substrate. Our coating provides the optimum combination to suppress the initial Mg degradation and to promote cell growth on the coating surface by adjusting the vaterite content in the composite.

1. Introduction

Recently, magnesium and its alloys have attracted attention in the metallic biomaterials field because of their biodegradability and good mechanical properties [1-6]. They have a low Young's modulus of 41–45 GPa comparable to human cortical bone [1]. When Mg or Mg alloys are used in materials for implants, bone resorption should be avoided near the alloy.

After implantation of Mg into the living body, the following reaction follows:

$$Mg+2H_2O \rightarrow Mg(OH)_2 + H_2\uparrow . \quad (1)$$

This reaction proceeds rapidly since it contacts body fluids. Because of this corrosion reaction, the pH of the fluid near the Mg sample surface increases, generating H_2. The accumulation of H_2 gas in the soft tissue surrounding the Mg sample was observed within a week after implantation [2]. The local pH increase near the sample surface is harmful to the surrounding tissue. Following Mg corrosion, the sample surface was covered with corrosion products such as magnesium hydroxide, magnesium phosphate and magnesium carbonate. Precipitation of calcium phosphate was also reported because of the increase in the pH of the body fluid surrounding the implanted sample [2]. Formation of these insoluble salts at the sample surface retards the corrosion of the Mg sample.

The suppression of Mg corrosion at the initial stage of implantation plays an important role for biomedical applications. To control Mg corrosion, the Mg sample has been coated with a biodegradable polymer [7, 8]. Films of poly(L-lactic acid) (PLLA) and poly(ε-caprolactone) (PCL) less than 1 μm thick and without pores were effective in reducing the initial degradation rate of Mg and to improve its cytocompatibility [7]. However, detachment of the PCL film from the Mg substrate was observed. This was

probably because of H_2 gas generation between the polymer film and the substrate [7]. The porosity of the biodegradable polymer coating is important for controlling the degradation of the Mg substrate [8].

Besides control of the degradation, biodegradable Mg devices used as substitute materials for bone must be bioactive to stimulate bone growth [9, 10]. Surface coating techniques using calcium phosphate ceramics such as hydroxyapatite have been used to prepare bioactive layers on the Mg surface [11, 12]. Biodegradable polymer-based materials are likely candidates for coating the Mg substrate for this purpose. One way to form an ideal coating of Mg and its alloys is to form a layer consisting of biodegradable PLLA-based materials that are bioactive and can control the degradation of the Mg substrate.

Bioactive poly($_L$-lactic acid)-based composites containing calcium carbonate (vaterite) particles (PVCs) have been developed [13-15]. Vaterite is a polymorph of calcium carbonate and can be precipitated as submicrometer-sized secondary particles comprising several tens of nanometer-sized primary particles using a carbonation process. Vaterite particles with these shapes are expected to be highly soluble, releasing calcium ions to induce bone formation. When a PVC-coated Mg substrate is implanted into the body, vaterite can dissolve in the body fluid, making micrometer-sized pores on the coating surface after a certain period of time. This would aid in controlling the degradation of the Mg substrate. The composite coating could initially suppress the substrate degradation to improve the cytocompatibility. The pores of the coating also maintain the degradation of the substrate to prevent H_2 gas accumulation beneath the coating. Here, PVC coatings were applied to a Mg substrate to control the initial rapid degradation and improve the cytocompatibility.

2. Materials and methods

2.1. Sample preparation

A Mg rod (99.95%, 9.5 mm in diameter, Nilaco Corp., Japan) was employed in the present study. The impurities in the rod were 0.005 wt % of Zn, 0.032 wt % of Al, 0.016 wt % of Si, 0.001 wt % of Cu, 0.015 wt % of Mn, 0.006 wt % of Fe and 0.001 wt % of Ni. The rod was cut into 2.5 mm thick disks for use as substrates and polished with a #1200 (15 μm) SiC abrasive paper (Noritake Coated Abrasive Co. Ltd, Japan). The disks were washed in an ultrasonic bath in acetone for 10 min. All of the Mg samples were embedded with methyl methacrylate resin (Technovit 4004, Heraeus Kulzer, Germany) except for the top surfaces. The specimens obtained were 15 mm in diameter and 5 mm in thickness.

Two types of PVCs, containing 30 and 60 wt % vaterite, were prepared by a melt blending method at 180 °C for 10 min using poly(L-lactic acid) (PLLA) (LACEA®, molecular weight; 120 kDa, crystallinity; ~40 %, Mitsui Chemicals Inc., Japan) and vaterite particles (0.5 μm in diameter, Yabashi Industries Co. Ltd., Japan) as starting materials. The prepared materials are referred to as PVC*x* (*x*=30, 60). The molecular weights of the PLLA components in the composites were measured using gel permeation chromatography (GPC; LC-20, Shimadzu Corp., Japan). The crystallinity of the composites was determined using differential scanning calorimetry (DSC; DSC-8230, Rigaku, Japan) [16].

Each PVC sample was dissolved in chloroform to obtain a solution for spin-coating. The PLLA component of PVC in each solution was 4 wt %. One hundred μL of PVC solution was dropped onto the top surface of the Mg disk in the resin and the disk was

spin-coated at 5000 rpm for 90 s. It was confirmed prior to coating that the resin did not dissolve in chloroform. The uncoated Mg disk in the resin, referred to as "uncoated", was used as a control sample. The disk in resin, coated with PLLA by the same melt blending method without vaterite, was also prepared.

The top surface and cross section of the samples were observed using a scanning electron microscope (FE-SEM, JSM-6301F, JEOL, Japan) equipped with an energy dispersive X-ray spectrometer (EDX). The average surface roughness (Ra) of the coated surface was examined using a surface roughness tester (SURFCOM 1400-D, Tokyo Seimitsu Co. Ltd., Japan). The bonding strength between the PVC-coating layer and the Mg substrate was measured using a tensile testing machine (AGS-H, Shimadzu Corp., Japan). Aluminum shafts (diameter: 6.0 mm) were glued with an epoxy adhesive (Araldite® Rapid, Huntsman Advanced Materials, Japan) on the top and bottom surfaces of the Mg disks that were not embedded in the resin. After resting for 24 h for solidification of the adhesive, the supporting shaft glued on the top surface was pulled up at a tensile rate of 1.0 mm/min. At least five samples were tested for each coating.

2.2. Immersion in a cell culture medium

The uncoated Mg disks and the PLLA or PVC-coated samples embedded in resin were sterilized using ethylene oxide gas (EOG). Each sample was immersed in 27.5 mL of α-modified minimum essential medium (α-MEM, 1031120, Wako Pure Chemical Industries, Ltd., Japan) supplemented with 10 % v/v fetal bovine serum (FBS), abbreviated here as α-MEM+FBS. The α-MEM+FBS simulates human body fluid as previously reported [17]. An average adult human has about 2.75 L of blood plasma, and for this experiment the scale was reduced to 1/100 of the total capacity of an adult

human. The samples were then incubated in 5 % v/v CO_2 at 37 °C for 1, 3 or 7 days. To estimate the degradation rate of the substrate and the coating layer, the concentration of Mg^{2+}, Ca^{2+} and P^{5+} ions in the α-MEM+FBS were measured using inductively coupled plasma atomic emission spectroscopy (ICP-AES; ICPS-500, Shimadzu Corp., Japan). The experiment was performed in triplicate. The change in the amount of ions was given by the following equation:

$$R_x = [(C_{xs} - C_{x0}) \times 27.5] / A, \quad (2)$$

where R_x is the amount of ion x released from the sample, C_{x0} and C_{xs} are the concentrations of the ion x in α-MEM+FBS before and after immersion, respectively, and A is the sample top surface area.

The top surface of each sample was observed using an optical microscope (BIOREVO BZ-9000, Keyence Corp., Japan) and FE-SEM after immersion in α-MEM+FBS. To examine the amount of precipitate on the samples, EDX analysis was also performed over an area of 100 × 100 μm^2 for the samples immersed for 1, 3 or 7 days in α-MEM+FBS. Samples were analyzed in at least five different positions for each type of coating.

2.3. Cell proliferation assay

Murine osteoblast-like cells MC3T3-E1 (passage 18) were seeded on the samples sterilized with EOG in a culture dish with 27.5 mL of α-MEM+FBS with a density of 6,000 cells/mL, which equates to 16.5 × 10^4 cells/dish. The dishes were placed in a CO_2 incubator for 1, 3 or 7 days. A 1 mL portion of the supernatant was then poured into a 24 well microplate and each sample was transferred from the culture dish to the well of the microplate. Cell proliferation was determined using the WST-8 assay with Cell

Counting Kit-8 (CCK-8, Dojindo Laboratories, Japan). The CCK-8 solution is a tetrazolium compound, which is reduced by living cells into a colored formazan product. A 100 μL portion of the prepackaged CCK-8 solution was poured into each of the wells. The microplate was then placed in a CO_2 incubator for 2 h. The number of viable cells on the samples was estimated by measuring the absorbance of the resulting media at 450 nm with a microplate scanning spectrophotometer (SUNRISE Remote, Tecan Japan Co. Ltd., Japan). The strength of the absorbance signal of formazan product measured at 450 nm was directly proportional to the number of living cells. Cell culture tests were conducted in triplicate. The effect on the cytocompatibility of resin samples without a Mg disk was also examined.

2.4. pH measurements

Each sample was soaked in 27.5 mL of α-MEM+FBS and kept in a CO_2 incubator for 4 days after sterilization. During incubation, the pH of the medium near the sample surface was measured using a pH meter (TPX-999i, Toko Kagaku Kenkyusho Co. Ltd., Japan). The pH electrode was set to 1 mm from the top surface of the sample.

3. Results and Discussion

3.1. Properties of PVC*x*-coating layers

The thickness of the coating layers was estimated from cross-sectional SEM images of the samples. PLLA-, PVC_{30}-, and PVC_{60}-coating layers were determined to be 1.8, 2.0, and 3.0 μm thick, respectively. The thickness of the coating layers prepared by spin-coating is related to the concentration and the viscosity of the coating solution [18].

The vaterite content in the PVC solution was proportional to the thickness of the coating layer. The viscosity of the PVC solutions increased with increasing vaterite content in the PVC.

Figure 1 shows the SEM images of the coated surfaces. Almost no micrometer sized pores can be seen on the PLLA-coated or PVC_{30}-coated surfaces. However, some 0.5–1-μm diameter pores were observed on the PVC_{60}-coated surface. This may be because of the relatively low amount of PLLA matrix for the high content of vaterite in PVC_{60}.

The molecular weights of the PLLA component in the PLLA, PVC_{30} and PVC_{60} samples after melt blending were estimated to be 90, 76 and 46 kDa, respectively. In addition, the PLLA polydispersity in the PLLA, PVC_{30} and PVC_{60} samples after melt blending was estimated to be 1.7, 2.1 and 2.8, respectively. The amount of crystallinity in the PLLA, PVC_{30} and PVC_{60} samples after melt blending was 15, 13 and 11%, respectively. Melt blending reduced the molecular weight of the polymer component and increased its polydispersity. The higher vaterite content also gave a lower molecular weight. Our previous report [14], suggested that the calcium ions in the vaterite coordinated with the carboxy groups in PLLA and formed a coordination bond. The cleavage of the PLLA chain might occur by melt blending, and subsequently form a coordination bond. A higher vaterite content may result in a lower molecular weight. The difference in the molecular weights may influence the degradation of the materials used for coating and therefore that of the Mg substrate.

The average surface roughness of the uncoated, PLLA-, PVC_{30}- and PVC_{60}-coated surfaces was 0.12, 0.08, 0.15 and 0.20 μm, respectively. PVC_{30} and PVC_{60} tended to have a slightly higher surface roughness; however there were no significant differences between the samples.

The bonding strengths of the coating layers and Mg substrate were approximately 0.8–1.0 MPa. There was no clear dependence on molecular weight, coating layer thickness or vaterite content. These values are slightly lower than the 2.5–4.0 MPa previously obtained for the PLLA and PCL coating layers prepared by spin-coating [7]. The free ends of the polymer chain are believed to provide free carboxy groups and form electrostatic intermolecular interactions with the Mg substrate surface. The difference in the bonding strength between the previous report and our results is probably due to the difference in molecular weights of the polymers used, and the polishing condition of Mg substrate resulting in a difference in the substrate surface roughness.

3.2. Degradation of uncoated and coated samples

Figure 2 shows optical micrographs of the sample surfaces after immersion in α-MEM+FBS for 7 days. Polishing marks were observed on all of the Mg substrates since the coating layers were semi-transparent and only a few micrometers thick. A large number of bright or dark spots were clearly observed on the whole surface of the uncoated sample. These are corrosion products or pits. Corrosion of the PLLA- and PVC_{30}-coated samples was observed locally. Coatings with PVC_{30} or PLLA appear effective in retarding corrosion of the Mg substrate. However, on the PVC_{60}-coated sample surface, corrosion products and pits were observed, similar to those observed on the uncoated sample. This suggests that the PVC_{60} coating was ineffective in suppressing the initial degradation of the Mg substrate.

Figure 3 shows SEM images of the surfaces of the coated samples after immersion in α-MEM+FBS for 7 days. There were a few pits of approximately 0.5–1.0 μm in

diameter on the PLLA- and PVC_{30}-coated surfaces. However, 1.0–2.0-μm diameter pores were observed on the PVC_{60}-coated surface., The formation of the larger pores on the PVC_{60}-coated surface probably relates to the lower molecular weight of the PLLA component and a higher concentration of vaterite particles than in the other coating materials (Fig. 3 (c)). The PLLA component with a low molecular weight degrades at an earlier stage of immersion, decreasing the pH of the surrounding solution and causing detachment of the vaterite particles from the coating layer. The higher vaterite concentration also encourages pore formation. This early degradation of the PLLA component and pore formation may accelerate the corrosion of the Mg substrate.

An image of the Mg^{2+} ions released into α-MEM+FBS during the immersion is shown in Fig. 4 (a). α-MEM+FBS initially contained 20 μg/mL of Mg^{2+} ions. The amount of Mg^{2+} ions released increased with immersion time. The Mg^{2+} ions released from the uncoated Mg sample reached more than 10 $\mu g/mm^2$ after 7 days of immersion. The sample with the PVC_{60}-coating released almost the same amount of Mg^{2+} ions as the uncoated Mg sample after a period of 3 days. After 7 days, higher amounts of Mg^{2+} ions were released from the sample with the PVC_{60}-coating than the uncoated Mg sample. This agrees with the observations made using optical and electron microscopy, suggesting the lower molecular weight component of the PLLA and a higher vaterite concentration accelerated the substrate degradation.

However, the PLLA- and PVC_{30}-coating caused the Mg substrate to degrade slowly over a period of 7 days. After 7 days, the amount of Mg^{2+} ions released was 2–3 $\mu g/mm^2$. The PLLA- and PVC_{30}-coating are suitable for the suppression of the Mg degradation under these experimental conditions. The coatings did not delaminate during immersion in α-MEM+FBS. This suggests that the coating layers are strongly bonded as a bonding

strength of 0.8–1.0 MPa. These bonding strengths were enough for avoiding the detachment of the coatings in these experimental conditions. However, it is necessary to evaluate the stability of the coating layers for a longer period of time with a longer immersion test.

Figure 4 (b) and (c) show the concentration of Ca^{2+} and P^{5+} ions in α-MEM+FBS over an immersion period of 7 days. α-MEM+FBS initially contained about 78.1 μg/mL of Ca^{2+} and 34.3 μg/mL of P^{5+}. There was no change in the Ca^{2+} and P^{5+} ion concentrations for the uncoated and PLLA-coated samples during immersion. The Ca^{2+} and P^{5+} ion concentrations in the PVC-coated samples decreased slightly in α-MEM+FBS with increasing immersion time. The decrease in the concentration may be because of the adsorption of these ions on the sample surface or the precipitation of insoluble salts such as calcium phosphate even though the precipitates were not observed on the surface of the sample or glass container with the naked eye.

The top surfaces of the samples were analyzed by EDX before and after immersion in α-MEM+FBS. The concentrations of Ca and P after immersion in α-MEM+FBS are shown in Figure 5. On the PVC_{30}-coated surface, the initial concentration of Ca and P atoms was 20.1 and 1.5 atom %, respectively. The PVC_{30}-coated surface had an increase in the Ca and P content with an increase in immersion time. The Ca/P ratio on the PVC_{30}-coating surface was 6.87 after immersion for 7 days. On the PVC_{60}-coated surface, the concentration of Ca and P atoms was initially 61.3 and 3.8 % respectively. The PVC_{60}-coated surface had a higher Ca content than the PVC_{30}-coated surface because of the higher vaterite content in the coating. There was no significant difference in the Ca content during immersion. However, the P content on the PVC_{60}-coated surface increased with the time. The Ca/P ratio on the PVC_{60}-coating surface was 6.71

after immersion for 7 days. Our previous work [13], demonstrated the usefulness of PVC for apatite formation in the simulated body fluid. The Ca/P ratios on the PVC_{30}- and PVC_{60}-coated surfaces were far from the stoichiometric Ca/P ratio of hydroxyapatite (1.67) since the Ca in the PVC_{30} and PVC_{60} films was also counted. It is possible that calcium phosphate compounds are formed on the PVC-coated surface by adsorbing P^{5+}. However, further investigation is needed to determine the details of the precipitates on the sample surfaces.

3.3. pH values near the sample surfaces

Figure 6 shows the pH of α-MEM+FBS near the sample surface after immersion of a period of up to 4 days. The initial pH of α-MEM+FBS in air was approximately 8.3. After 6 h in the CO_2 incubator, it decreased to 7.55 and was stable. This was because the CO_2 gas dissolved into the medium and dissociated in the incubator. The pH of the medium near the uncoated sample surface decreased to 7.7 after a few hours. It then slowly reached 7.8 after 4 days. Degradation of the Mg increased the pH of the medium. The pH of the medium near the PLLA-coated sample surface decreased to around 7.0. Near the surface of the PVC_{30}- and PVC_{60}-coated samples, the pH decreased to between 7.4 and 7.5. The low molecular weight PLLA component in these coatings may degrade at an early stage of immersion, inducing local acidification. However, the pH of the media near the PVC_{30}- or PVC_{60}-coated surface was higher than that of the PLLA-coated surface. This is probably because of the partial dissolution of the vaterite particles, which produces carbonate ions and buffers the medium. In the case of PVC-coated samples, the degradation of the PLLA component in the PVC-coated samples overcomes the effect of the OH^- generated by the Mg substrate degradation.

However, the carbonate ions derived from the vaterite buffered the medium, resulting in a pH of 7.4. This is closer to the pH of blood plasma, suggesting that PVC can maintain the pH balance of the medium with the degradation of PLLA and vaterite.

3.4. Cell proliferation

Figure 7 shows the cell proliferation of the MC3T3-E1 cells on the uncoated and coated samples. Using the WST-8 assay, it was confirmed that the absorbance of the formazan in the WST-8 reagent correlates with the number of viable cells [19, 20]. There were no significant differences in cell viability among the samples that were cultured for 1 day. After culturing the cells for 3 days, the number of viable cells on the coated samples was significantly higher than on the uncoated sample. The difference in cell viability between the samples was more obvious after 7 days of culture. The number of viable cells on the PVC-coated samples was significantly higher than on the PLLA-coated and uncoated samples. The PVC_{60}-coated samples had the greatest number of viable cells.

Surface roughness is a key factor for cell attachment and proliferation; however the surfaces employed in this study had a similar surface roughness of 0.08–0.20 μm. This could not explain the difference in the cell viability of the samples. Surface wettability is another important factor influencing cell attachment [21]. The average static contact angles of the uncoated, PLLA-, PVC_{30}- and PVC_{60}-coated surfaces were 61±2, 95±5, 75±3 and 72±4 degrees, respectively. The error is given by the standard deviation. The relatively high hydrophobicity of the PLLA-coated surface may correlate with the lower cell growth after 3 and 7 days of culture. The slightly lower contact angles of the

PVC-coated samples may relate to the amount of vaterite particles in the composites. This may contribute to higher cell growth after 3 and 7 days of culture.

It is possible that the ions released from the samples influenced cell proliferation. It was reported that Ca^{2+} ions released from the samples enhanced cell proliferation of osteoblasts [22, 23]. This implies that PVC coatings have an influence on cytocompatibility. However, the Ca^{2+} ion concentration in the α-MEM+FBS after the PVC_{30}-coated samples were immersed for 7 days was 137 μg/mL. The Ca^{2+} ion concentration when the PVC_{60}-coated samples were immersed in α-MEM+FBS was 134 μg/mL. There was almost no difference in the Ca^{2+} ion concentration in the α-MEM+FBS with different PVC-coated samples. Although the optimum concentration was not determined, Mg^{2+} ions were reported to stimulate cell attachment and proliferation of osteoblasts [24, 25]. The PVC_{60}-coated samples had the highest concentration of released Mg^{2+} ions (Fig. 4). This suggests that Mg^{2+} ions promote cell proliferation. However, the cells could not proliferate sufficiently on the uncoated sample, which released a similar concentration of Mg^{2+} ions to the PVC_{60}-coated samples. The stability of the surface structures under biological conditions is a key consideration for cytocompatibility [26]. The surface of the uncoated sample had some instability because of the high reactivity of Mg (Fig. 3 (a)). The effect of the pH of the medium on cell behavior was previously reported [27, 28]. The higher pH of α-MEM+FBS near the uncoated sample surface may inhibit cell growth on the sample surface. The lower pH near the PLLA-coated sample surface is lower than that of human blood plasma (7.4), and may also suppress the cell growth on the sample surface.

4. Conclusion

To control the rapid degradation of Mg and improve its cytocompatibility, two types of poly(L-lactic acid)/vaterite composite materials (PVCs) were coated on the Mg substrate. The surface of the PVC_{30}-coated sample had no pores and the coating was maintained after immersion in α-MEM+FBS for 7 days, suppressing the degradation of the Mg substrate. A large number of 1.0–2.0-μm diameter pores were observed on the PVC_{60}-coated surface. This coating had no effect on the suppression of the Mg substrate degradation, probably because of the pores in the coating. The pH of α-MEM+FBS near the coatings remained close to that of human body fluid. This might be because of the degradation of the PLLA matrix, the amount of dissolution of vaterite from the PVC and the degradation of the Mg substrate. The number of cells of MC3T3-E1 on the PVC_{60}-coated sample was higher than on the PLLA- and PVC_{30}-coated sample. The $Ca^{2+}$and Mg^{2+} ions that originated from the samples and the stability of the surface structures are believed to have influenced the cell proliferation. The degradation rate and the cell viability of the PVC-coated surface on the Mg substrate were controlled by the vaterite content of the PVC. Based on the results, the PVC-coating containing 30 wt % vaterite can suppress the degradation of the Mg substrate and enhance the proliferation of osteoblast-like cells. PVC coatings on Mg and its alloys may be effective for preparing new types of biodegradable metallic bone plates or screws.

Acknowledgements

The authors thank Dr. Hirotaka Maeda for helpful discussions. This work was supported in part by the Institute of Ceramics Research and Education (ICRE), Nagoya

Institute of Technology.

References

1. Staiger MP, Pietak AM, Huadmai J, Dias G. Magnesium and its alloys as orthopedic biomaterials: A review. Biomaterials. 2006;27:1728–34.

2. Witte F, Kaese V, Haferkamp H, Switzer E, Meyer-Lindenberg A, Wirth CJ, Windhagen H. In vivo corrosion of four magnesium alloys and the associated bone response. Biomaterials. 2005;26:3557–63.

3. Witte F, Hort N, Vogt C, Cohen S, Kainer KU, Willumeit R, Feyerabend F. Degradable biomaterials based on magnesium corrosion. Current Opinion in Solid State and Mater. Sci. 2008;12:63–72.

4. Witte F. The history of biodegradable magnesium implants: A review. Acta Biomater. 2010;6:1680–92.

5. Zeng R, Dietzel W, Witte F, Hort N, Blawert C. Progress and challenge for magnesium alloys as biomaterials. Adv. Eng. Biomater. 2008;10:B3–14.

6. Mueller WD, Nascimento ML, Lorenzo de Mele MF. Critical discussion of the results from different corrosion studies of Mg and Mg alloys for biomaterial applications. Acta Biomater. 2010;6:1749–55.

7. Xu L, Yamamoto A. Characteristics and cytocompatibility of biodegradable polymer film on magnesium by spin coating. Colloids and Surface B: Biointerfaces. 2012;93:67–74.

8. Wong HM, Yeung KWK, Lam KO, Tam V, Chu PK, Luk KDK, Cheung KMC. A

biodegradable polymer-based coating to control the performance of magnesium alloy orthopaedic implants. Biomaterials. 2010;31:2084–96.

9. Hubbell JA. Bioactive biomaterials. Current Opinion in Biotech. 1999;10:123–9.

10. Kokubo T, Kim HM, Kawashita M. Novel bioactive materials with different mechanical properties. Biomaterials. 2003;24:2161–75.

11. Hiromoto S, Yamamoto A. High corrosion resistance of magnesium coated with hydroxyapatite directly synthesized in an aqueous solution. Electrochemica Acta. 2009;54:7085–93.

12. Song YW, Shan DY, Han EH. Electrodeposition of hydroxyapatite coating on AZ91D magnesium alloy for biomaterial application. Mater. Lett. 2008;62:3276–9.

13. Maeda H, Kasuga T, Nogami M, Hibino Y, Hata K, Ueda M, Ota Y. Biomimetic apatite formation on poly(lactic acid) composites containing calcium carbonates. J. Mater. Res. 2002;17:727–30.

14. Kasuga T, Maeda H, Kato K, Nogami M, Hata K-I, Ueda M. Preparation of poly(lactic acid) composites containing calcium carbonate (vaterite). Biomaterials. 2003;24:3247–53.

15. Maeda H, Kasuga T, Hench LL. Preparation of poly(L-lactic acid)-polysiloxane calcium carbonate hybrid membranes for guided bone regeneration. Biomaterials. 2006;27:1216–22.

16. Chen HL, Hwang JC. Some comments on the degree of crystallinity defined by the enthalpy of melting. Polymer. 1995;36:4355–57.

17. Yamamoto A, Hiromoto S. Effect of inorganic salts, amino acids and proteins on the degradation of pure magnesium in vitro. Mater. Sci. Eng. C. 2009;29:1559–68.

18. Schubert DW, Dunkel T. Spin coating from a molecular point of view: its

concentration regimes, influence of molar mass and distribution. Mater. Res. Innovat. 2003;7:314–21.

19. Ishiyama M, Miyazono Y, Sasamoto K, Ohkuwa Y, Ueno K. A highly water-soluble disulfonated tetrazoloum salt as a chromogenic indicator for NADH as well as cell viability. Talanta. 1997;44:1299–1305.

20. Tominaga H, Ishiyama M, Ohseto F, Sasamoto K, Hamamoto T, Suzuki K, Watanabe M. A water-soluble tetrazolium salt useful for colorimetric cell viability assay. Anal. Commun. 1999;36:47–50.

21. Lampin M, Warocquier-Clerout R, Legris C, Degrange M, Sigot-Luizard MF. Correlation between substratum roughness and wettability, cell adhesion, and cell migration. J. Biomed. Mater. Res. 1997;36:99–108.

22. Webster TJ, Ergun C, Doremus RH, Siegel RW, Bizios R. Enhanced functions of osteoblasts on nanophase ceramics. Biomaterials. 2000; 21:1803–10.

23. Maeno S, Niki Y, Matsumoto H, Morioka H, Yatabe T, Funayama A, Toyama Y, Taguchi T, Tanaka J. The effect of calcium ion concentration on osteoblast viability, proliferation and differentiation in monolayer and 3D culture. Biomaterials. 2005;26:4847–58.

24. Zreiqat H, Howlett CR, Zannettino A, Evans P, Tanzil GS, Knabe C, Shakibaei M. Mechanisms of magnesium-stimulated adhesion of osteoblastic cells to commonly used orthopaedic implants. J. Biomed. Mater. Res. 2002;62:175–84.

25. Yamasaki Y, Yoshida Y, Okazaki M, Shimazu A, Kubo T, Akagawa A, Hamada Y, Takahashi J, Matsuura N. Synthesis of functionally graded $MgCO_3$ apatite accelerating osteoblast adhesion. J. Biomed. Mater. Res. 2002;62:99–105.

26. Puleo DA, Nanci A. Understanding and controlling the bone-implant interface.

Biomaterials. 1999;20:2311–21.

27. Kohn DH, Sarmadi M, Helman JI, Krebsbach PH. Effects of pH on human bone marrow stromal cells *in vitro*: Implications for tissue engineering of bone. J. Biomed. Mater. Res. 2002;60:292–9.

28. Arnett TR. Extracellular pH regulates bone cell function. J. Nutr. 2008;138:4155–85.

Figure Captions

Fig. 1 SEM images of (a) the PLLA-coated sample, (b) the PVC_{30}-coated sample and (c) the PVC_{60}-coated sample.

Fig. 2 Optical images of the surface of the samples after immersion in α-MEM+FBS for 7 days: (a) uncoated sample; (b) PLLA-coated sample; (c) PVC_{30}-coated sample; (d) PVC_{60}-coated sample.

Fig. 3 SEM images of the coated surfaces after immersion in α-MEM+FBS for 7 days: (a) PLLA-coated sample; (b) PVC_{30}-coated sample; (c) PVC_{60}-coated sample.

Fig. 4 (a) The amount of Mg^{2+} ions released from the sample into α-MEM+FBS (b) the amount of Ca^{2+} ions and (c) the amount of P^{5+} ions in α-MEM+FBS after immersion of (○) the uncoated sample, (◇) PLLA-coated sample, (■) PVC_{30}-coated sample and (▲) the PVC_{60}-coated sample.

Fig. 5 Percentage of Ca and P atoms on the (a) PVC_{30}-coated surface and (b) PVC_{60}-coated surface after immersion in α-MEM+FBS.

Fig. 6 Change in the pH of α-MEM+FBS during incubation in 5 % v/v CO_2 at 37 °C after soaking: (a) α-MEM+FBS only; (b) uncoated sample; (c) PLLA-coated sample; (d) PVC_{30}-coated sample (e) PVC_{60}-coated sample.

Fig. 7 Absorbance as a function of the number of cells on each sample after culturing the MC3T3-E1 cells (* $p < 0.05$ as compared using the student's *t*-test).

Figures

Fig. 1

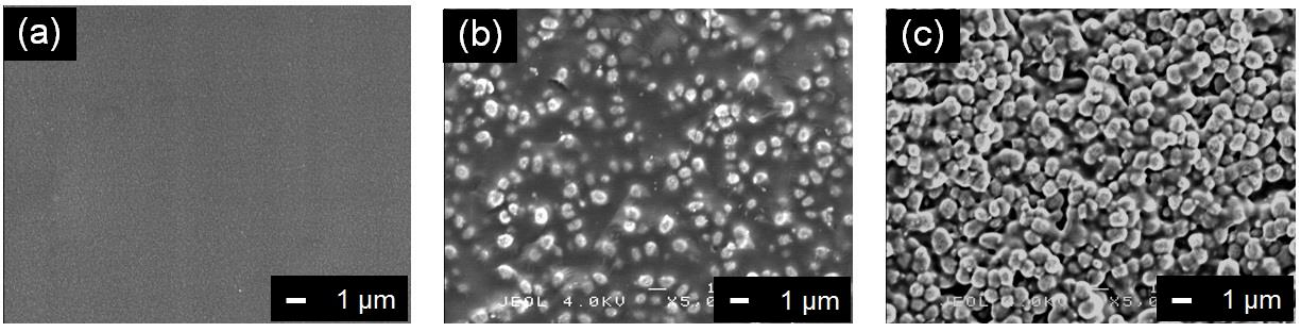

Fig. 2

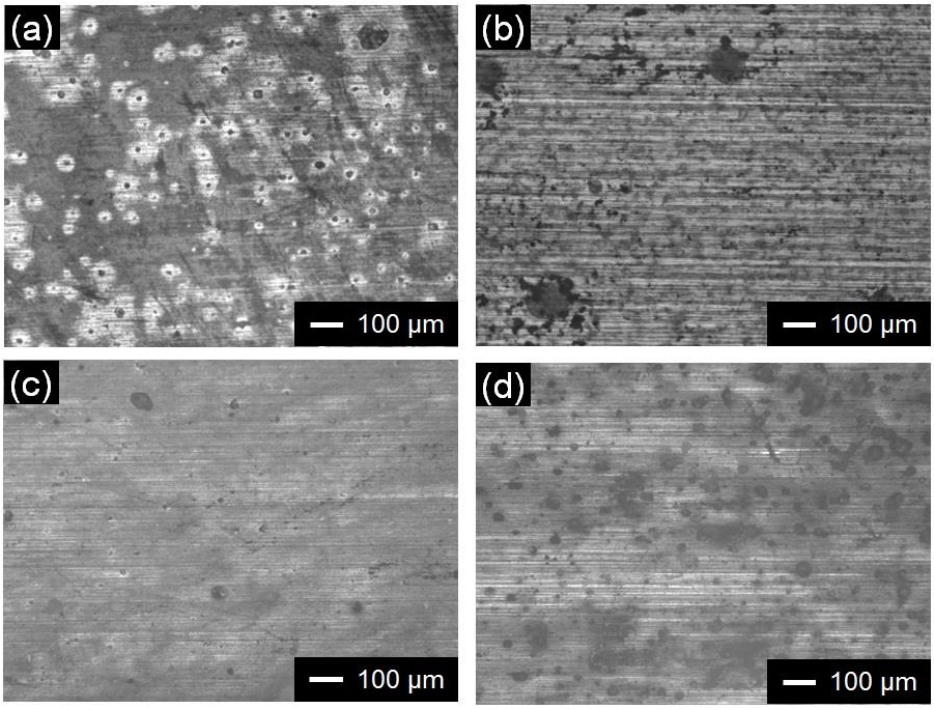

Fig. 3

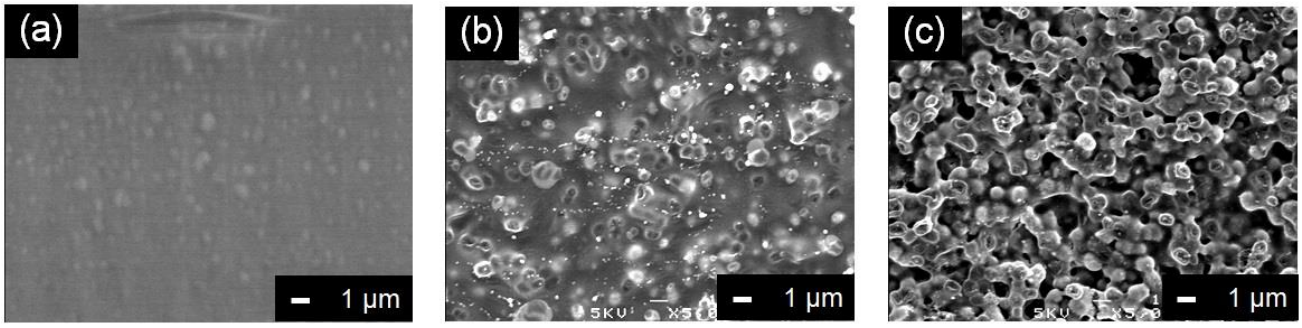
(a)
1 μm
(b)
1 μm
(c)
1 μm

Fig. 4

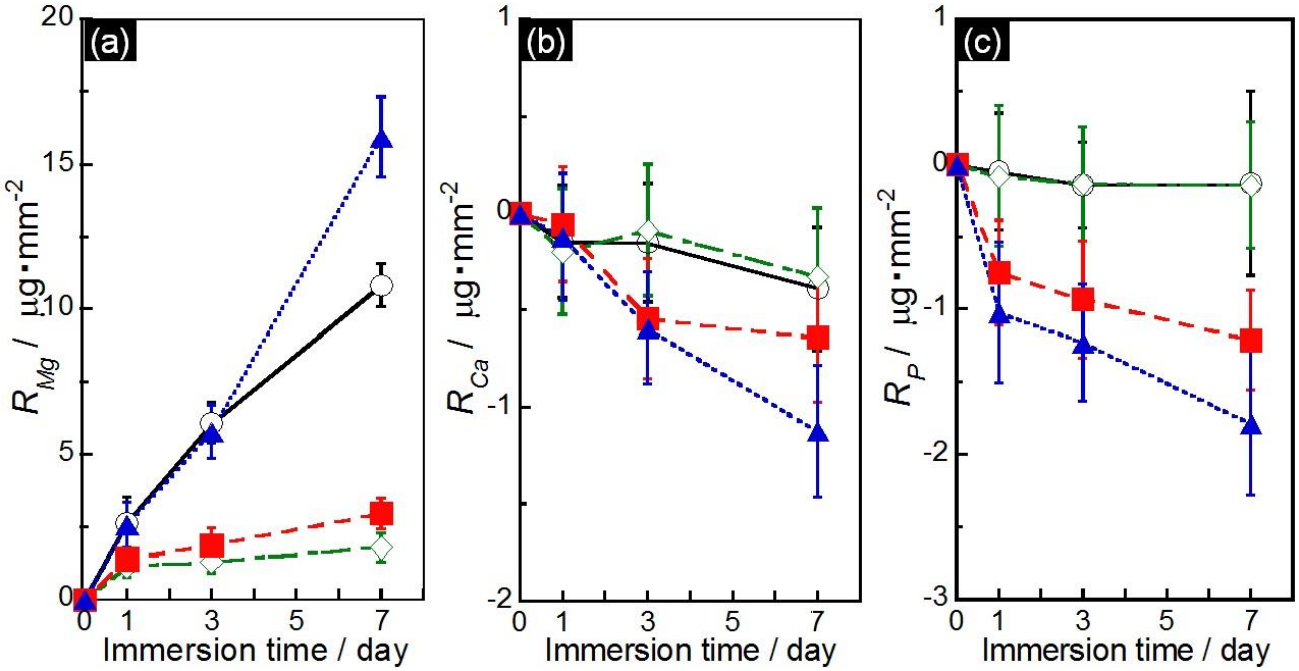
(a)
R_{Mg} / μg·mm^{-2}
Immersion time / day
(b)
R_{Ca} / μg·mm^{-2}
Immersion time / day
(c)
R_P / μg·mm^{-2}
Immersion time / day

Fig. 5

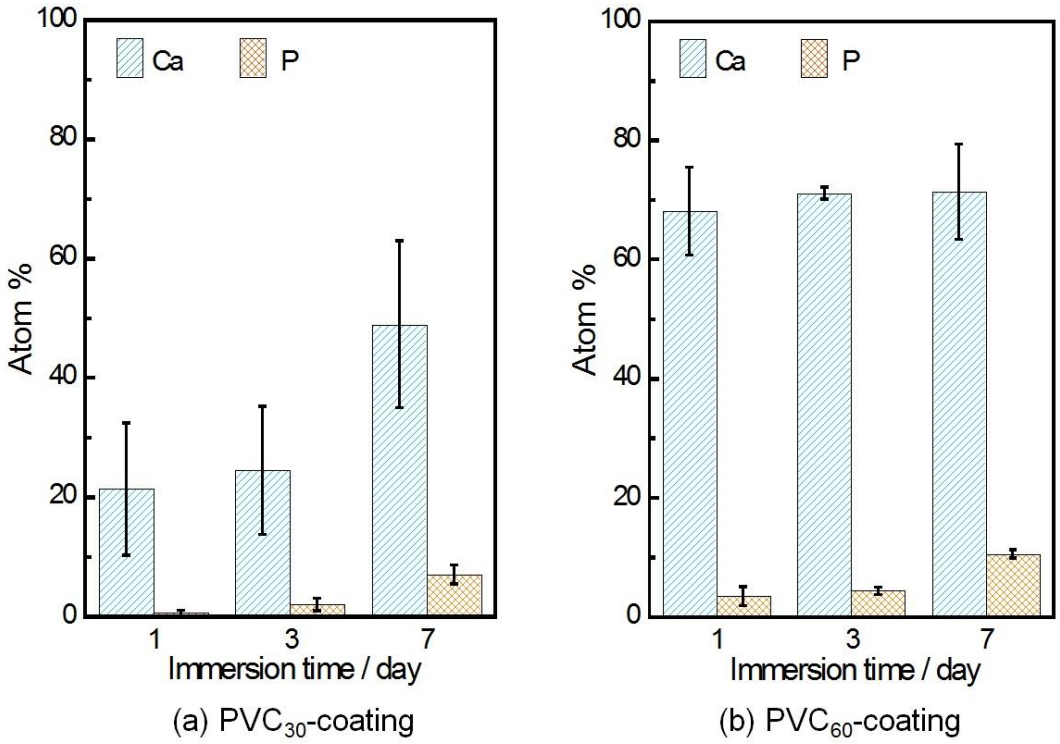
Ca
P
Atom %
Immersion time / day
(a) PVC30-coating
(b) PVC60-coating

Fig. 6

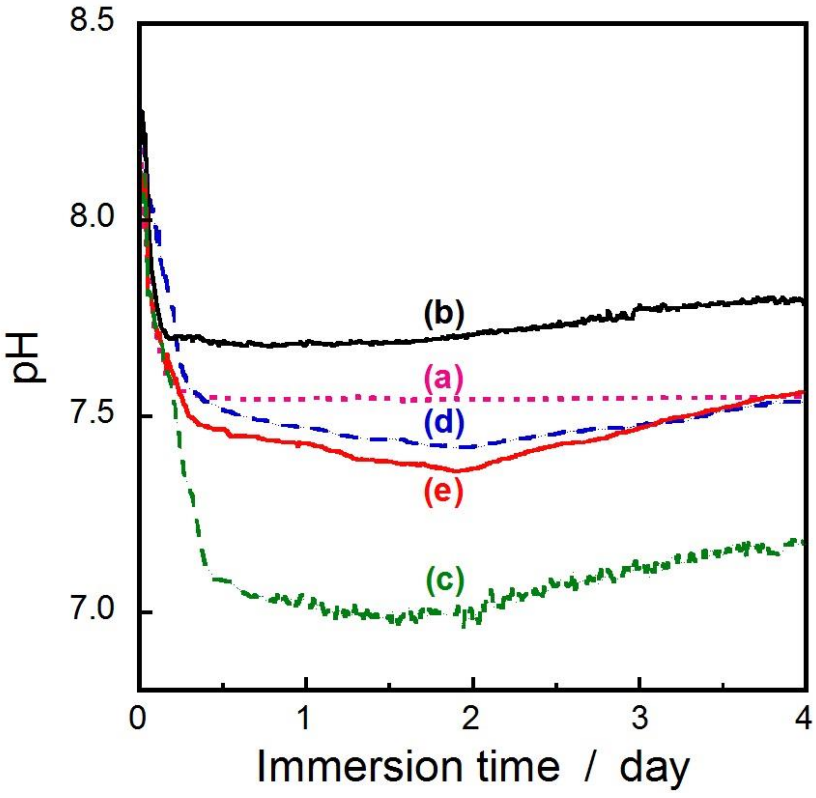
pH
Immersion time / day
(a)
(b)
(c)
(d)
(e)

Fig. 7

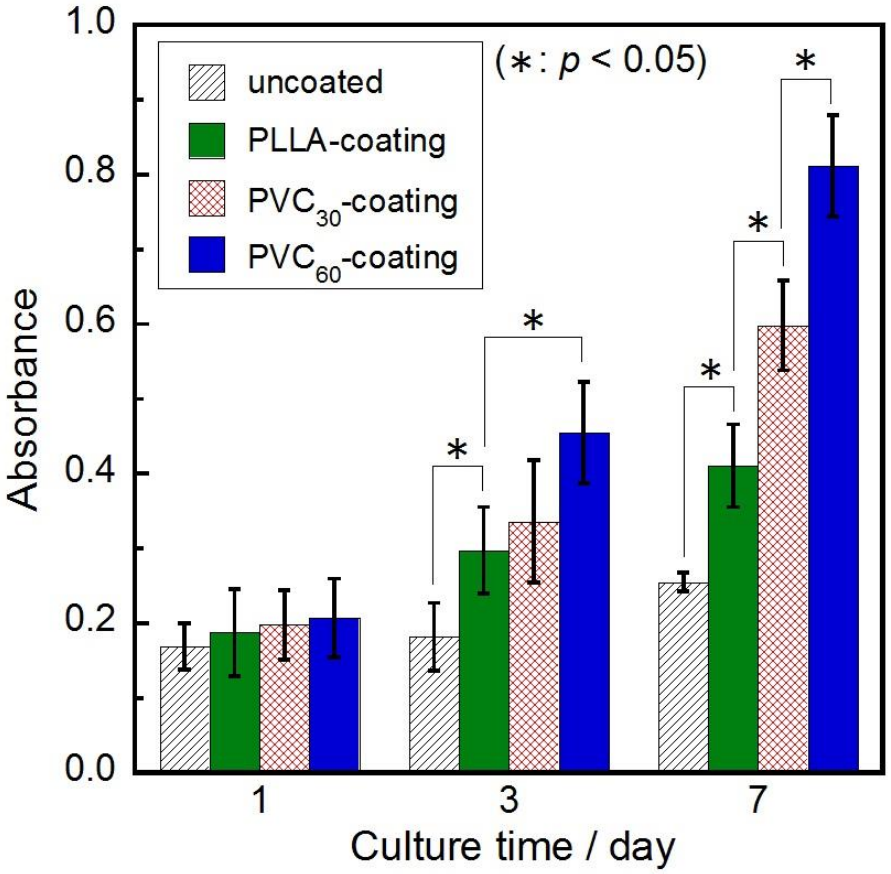
1.0
0.8
0.6
0.4
0.2
0.0
Absorbance
uncoated
PLLA-coating
PVC30-coating
PVC60-coating
(∗: p < 0.05)
∗
∗
∗
∗
1
3
7
Culture time / day